International Journal of Concrete Structures and Materials
Vol.8, No.2, pp.157–164, June 2014
DOI 10.1007/s40069-013-0063-y
ISSN 1976-0485 / eISSN 2234-1315

Durability Properties and Microstructure of Ground Granulated Blast Furnace Slag Cement Concrete

Bahador Sabet Divsholi*, Tze Yang Darren Lim, and Susanto Teng

(Received April 29, 2013, Accepted December 4, 2013)

Abstract: Ground granulated blast-furnace slag (GGBS) is a green construction material used to produce durable concrete. The secondary pozzolanic reactions can result in reduced pore connectivity; therefore, replacing partial amount of Portland cement (PC) with GGBS can significantly reduce the risk of sulfate attack, alkali–silica reactions and chloride penetration. However, it may also reduce the concrete resistance against carbonation. Due to the time consuming process of concrete carbonation, many researchers have used accelerated carbonation test to shorten the experimental time. However, there are always some uncertainties in the accelerated carbonation test results. Most importantly, the moisture content and moisture profile of the concrete before the carbonation test can significantly affect the test results. In this work, more than 200 samples with various water–cementitious material ratios and various replacement percentages of GGBS were cast. The compressive strength, electrical resistivity, chloride permeability and carbonation tests were conducted. The moisture loss and microstructure of concrete were studied. The partial replacement of PC with GGBS produced considerable improvement on various properties of concrete.

Keywords: blended cement, durability, GGBS, chloride penetration, concrete, carbonation, durability.

1. Introduction

Manufacturing Portland cement (PC) is a major contributor of greenhouse gases, responsible for about 5 % of all global carbon dioxide emissions (Habert and Roussel 2009). In comparison, the production of ground granulated blast-furnace slag (GGBS) requires less than a fifth of the energy and produces less than a tenth of the carbon dioxide emissions. It is well known that blast furnace slag cement (BFSC) has been manufactured by integrating GGBS with cement clinker or by separate grinding (Wang et al. 2005). For a long period of time, the application of GGBS was limited to the production of BFSC. Due to its less grindability, the surface area of the produced BFSC was even lower than that of commercial PC and its reactivity was limited. With advancement in technology, finer GGBS (particle size less than 10 μm) with increased reactivity was produced. The secondary pozzolanic reactions can result in reduced pore connectivity in the concrete. Therefore, partial replacement of PC with GGBS can significantly reduce the risk of sulfate attack, alkali–silica reactions and chloride penetration and increase compressive strength (Güneyisi and Gesoğlu 2008; Hadj-Sadok et al. 2010; Nazari and Riahi 2011; Shi et al. 2011, 2012; Teng et al. 2013). However, it may reduce the resistance of the concrete against carbonation (Harrison et al. 2012; Shi et al. 2009; Jia et al. 2011).

Concrete carbonation is one of the most important phenomena affecting the durability of concrete. Concrete carbonation has been studied extensively over the last few decades. However, due to the time consuming process of carbonation, many researchers have used accelerated carbonation test to shorten the experimental time. Considering the complex process of carbonation and the number of parameters involved, there are always some uncertainties in the accelerated carbonation test results. Most importantly, the moisture content and moisture profile of the concrete before the carbonation test can significantly affect the test results. The CO_2 from the environment will dissolve in the pore solution through the partially filled pore system and will react with the cement hydration products. If the concrete is fully saturated, carbonation will be slow (Lagerblad 2005). Based on the quality of concrete and the environmental conditions, concrete will achieve equilibrium moisture profile status after several months (Sabet and Jong 2006). To shorten this time, various preconditioning techniques were employed before the carbonation test. Oven drying is one of the most popular methods. However, the high temperature drying can damage the pore structure of concrete (Galle 2001). Partial replacement of PC with supplementary cementitious materials (SCM) is known to reduce the resistance against carbonation due to consumption of calcium hydroxide during pozzolanic reactions. On the other hand, the finer pore structure and lower permeability due to SCM replacement results in higher degree of internal

School of Civil and Environmental Engineering, Nanyang Technological University, Singapore 639798, Singapore.
*Corresponding Author; E-mail: bsabet@ntu.edu.sg

saturation which may slow down the carbonation rate. This improvement may diminish as a result of artificial preconditioning which could damage the pore structure and lower the degree of internal saturation below the natural equilibrium for blended cement concrete. Therefore, the increased carbonation rate measured in accelerated carbonation test may not be the correct natural carbonation rate of blended cement concrete. Jia et al. (2011) also suggested that the accelerated carbonation method sometimes may 'enlarge' the influence of the mineral admixture content and change the dynamics of concrete in carbonation.

In this work, more than 200 samples with various water–cementitious material ratios (0.4, 0.5 and 0.6) and various replacement percentages of GGBS were cast. The compressive strength, electrical resistivity, chloride permeability and carbonation tests were conducted during 4 years of experimental study. The moisture loss was recorded by gravimetric technique and the microstructure of the concrete was investigated using the mercury intrusion porosimetry (MIP). The results showed that partial replacement of PC with GGBS contributed considerable improvement on various properties of concrete.

2. Experimental Work

The characteristic of GGBS was examined using particle size analyzer, X-ray diffraction (XRD) and chemical analysis tests. Table 1 shows the physical and chemical properties, whereas Figs. 1 and 2 show the particle size distribution and XRD test result of the GGBS respectively. The average particle size of GGBS was 9.2 μm compared to 14.6 μm for PC (type II). As shown in Fig. 2, no stand-out peak was detectable in the XRD results, representing no crystalline phase was detected. In additon, the GGBS had a high degree of reactivity. In this work, more than 200 samples with various water–cementitious material ratios (0.4, 0.5 and 0.6) and various replacement percentages of GGBS (0, 10, 30 and 50 %) were cast. Table 2 shows the concrete mix proportions.

The cube compressive strength test was completed using a 3,000 kN compression machine according to BS EN 12390-3 (2009). The mercury intrusion porosimeter 9400 Series was used to study the microstruture of concrete. The MIP gradually forces mercury into the pores of concrete from evacuated condition (50 μmHg pressure) to high pressure of about 60,000 Psia (Ji and Jong 2003). The MIP results were used to study the effect of GGBS replacement and preconditioning on the pore structure of concrete. The gravimetric weight loss of the concrete was studied in controlled drying condition at relative humidity of 75 % and temperature of around 28 °C. The drying rate of concrete after oven drying and re-wetting was also studied to demonstrate the effect of oven drying at 105 °C on microstructure of concrete.

To study the resistance of concrete against chloride penetration, the total charges passing through the concrete for the first 6 h were recorded every 30 min, simulating the rapid chloride permeability (RCP) test as described by ASTM C1202 (2010). In addition, the electrical resistivity of the concrete was measured. The electrical resistivity measurement is a criterion to classify the concrete according to the corrosion rate of the concrete. The electrical resistance has a correlation coefficient of above 0.93 with chloride penetration test (Lim et al. 2012). The four point Wenner probe is a commercially available equipment to measure the electrical resistivity of the concrete. Placing the Wenner probe on one exposed surface of the concrete, the probe produces a low frequency alternating electrical current passing between the two outer electrodes while the voltage drop between the two inner electrodes is measured. The apparent electrical resistivity ρ observed on the display is based on the following equation:

Table 1 Physical and chemical characteristics of PC and GGBS.

	Portland cement (II)	GGBS
Physical properties		
Blaine surface area (m^2/kg)	370	410
BET surface area (m^2/kg)	1,600	2,100
Mean particle diameter (μm)	14.7	9.2
Density (kg/m^3)	3,150	2,720
Chemical analysis (%)		
SiO_2	21	36
Al_2O_3	6	9
Fe_2O_3	4	1
CaO	63	44
SO_3	1	1
MgO	2	8

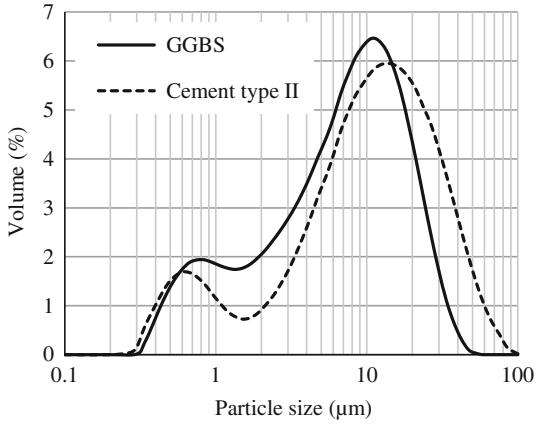

Fig. 1 Particle size distribution of GGBS and cement (II).

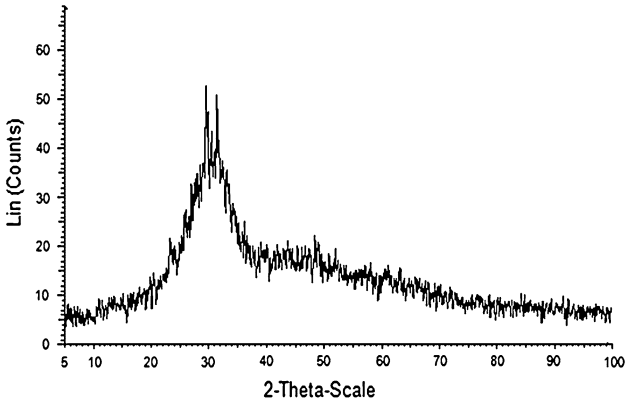

Fig. 2 X-ray diffraction test on GGBS.

$$\rho = 2\pi aV/I \quad (1)$$

where a is the spacing between the electrodes, V is the voltage drop, and I is the current passing through the two outer electrodes. This equation is valid for a homogenous semi finite volume of the material (Gjørv 2009). Both RCP and electrical resistivity tests are very sensitive to moisture content, therefore the samples were fully saturated before testing (Polder 2001). Finally, natural carbonation test was carried out in the span of 4 years to study the natural carbonation rate of GGBS-blended concrete. The carbonbation depth was measured with spraying phenolphetalein indicator to freshly cutted concrete surface.

3. Results and Discussions

Increased slump and fluidity was measured with the increase in GGBS replacement percentage. For water–cementitious material ratio (w/c) = 0.5 and aggregate/cementitious material ratio (a/c) = 3, the slump was increased by 20, 35 and 55 % for 10, 30 and 50 % GGBS replacement, respectively. Similar improvement was reported elsewhere (Gao et al. 2005) for the partial replacement of PC with GGBS.

3.1 Mechanical Properties

Figure 3 shows the compressive strength development for the control mix and the mixes with 10, 30 and 50 % GGBS replacement. Slight increase in compressive strength was observed at 28 days. Since the GGBS was finer than PC, similar compressive strength was achieved as early as 3 days of water curing. Similar results for concrete mixes with finer GGBS were reported in other studies (Feng et al. 2000; Sabet et al. 2012).

3.2 Microstructure of Concrete

Figure 4 shows the normalized average pore size diameter (left) and pore size distribution (right) measured by MIP test

Table 2 Concrete mix proportions.

Mix	w/c	a/c	GGBS (%)	Total cementitious materials (kg/m^3)
C1	0.5	3	0	514
C2	0.5	4	0	424
C3	0.5	5	0	365
C4	0.4	3	0	526
C5	0.4	4	0	438
C6	0.6	4	0	407
G1	0.5	3	10	501
G2	0.5	3	30	498
G3	0.5	3	50	497
G4	0.5	4	50	418
G5	0.6	4	50	402
G6	0.4	4	50	436

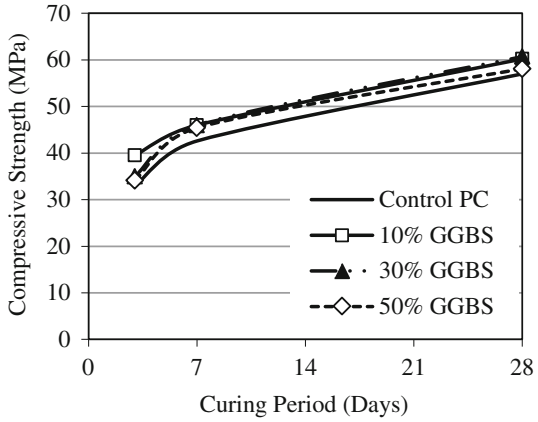

Fig. 3 Effect of GGBS replacement on compressive strength.

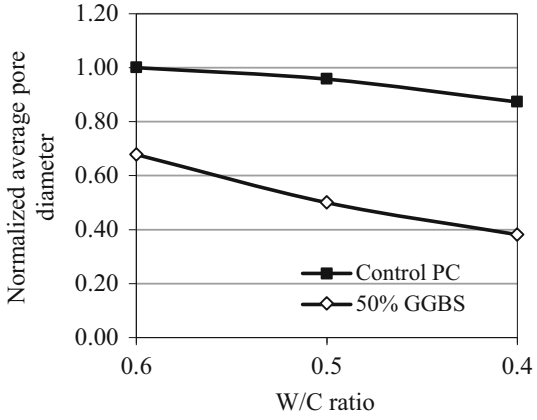

Fig. 5 Effect of w/c ratio on average pore diameter of concrete (at 28 days curing).

at 28 days of water curing. As shown, increasing the GGBS replacement percentage reduces the average pore size diameter by 15, 30 and 47 % for 10, 30 and 50 % GGBS replacement, respectively. Figure 5 shows the effect of w/c ratio and 50 % GGBS replacement on the normalized average pore size of concrete measured at 28 days of curing. In comparison, 50 % GGBS replacement at w/c ratio of 0.6 was more effective in reducing the average pore size than reducing w/c ratio from 0.6 to 0.4. The initial water curing for GGBS blended cement concrete was very important. As shown in Fig. 6, the normalized average pore size of GGBS blended cement was larger than that of the control PC mix after 1 day (right after demolding). However, the average pore size of GGBS blended cement significantly reduced with the increase in the water curing duration due to secondary pozzolanic reactions. As mentioned earlier, oven drying is commonly used for preconditioning of concrete samples before accelerated test in order to achieve the equilibrium condition (Galle 2001). Figure 7 shows the average pore size in the centre and near the surface of the samples after various drying condition. As shown, the average pore size increased significantly after 1 and 5 days of oven drying at 105 °C.

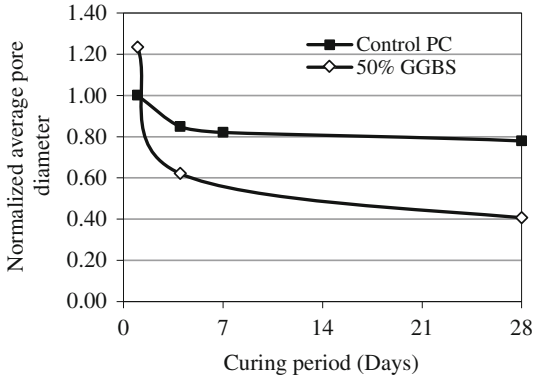

Fig. 6 Effect of curing duration on average pore diameter of concrete (w/c = 0.5).

3.3 Gravimetric Weight Loss and Pore Structure of Concrete

Figure 8 shows the effect of 10, 30 and 50 % GGBS replacement on the gravimetric weight loss compared to the PC concrete at 14 days of curing. As shown in Fig. 8, the rate of weight loss decreased with the increase in GGBS replacement. Figure 9 shows the effect of curing period on gravimetric weight loss for 50 % GGBS replacement compared to PC concrete. As shown, the total weight loss was

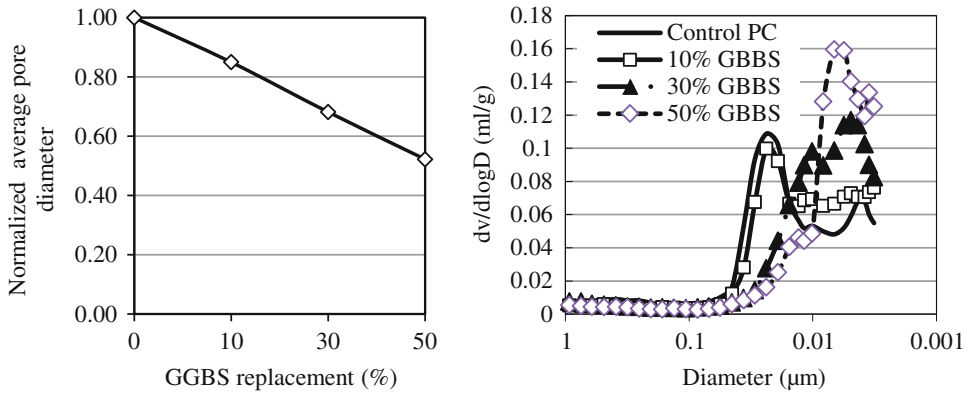

Fig. 4 Effect of GGBS replacement on average pore diameter of concrete (w/c = 0.5 at 28 days of water curing) (*left*), pore size distribution (*right*).

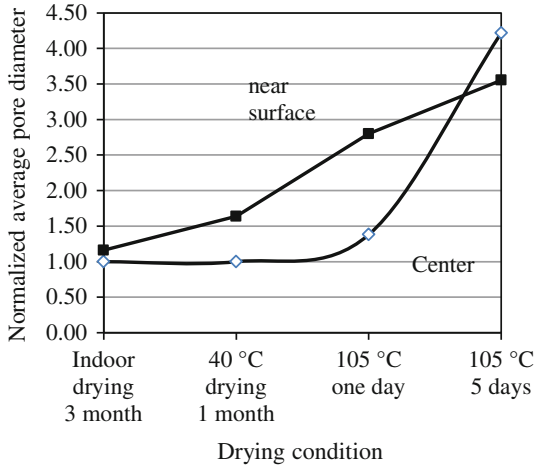

Fig. 7 Effect of drying condition on average pore diameter of PC concrete.

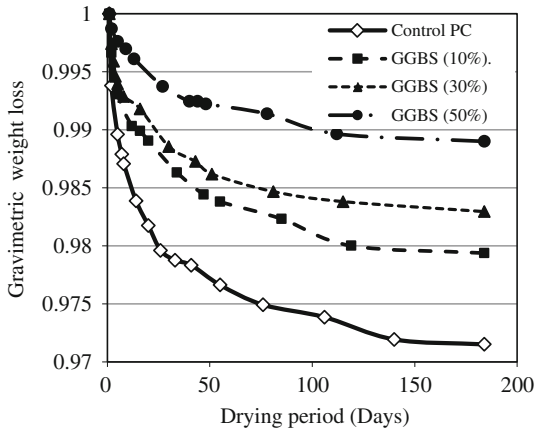

Fig. 8 Effect of GGBS replacement on gravimetric weight loss.

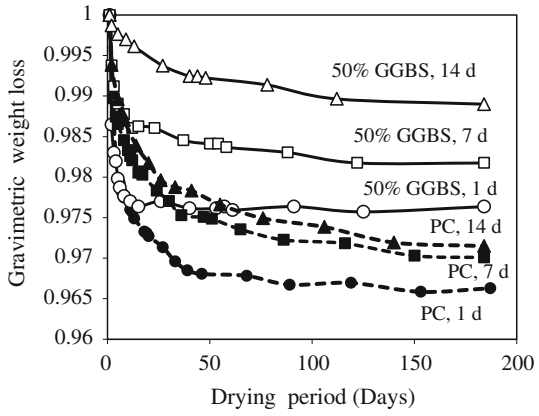

Fig. 9 Effect of curing and 50 % GGBS replacement on gravimetric weight loss.

much smaller and therefore the degree of internal saturation was higher for the concrete samples with GGBS replacement.

The oven drying at 105 °C not only increased the average pore size but it may also increase the pore connectivity. Therefore, after 5 days of oven drying, the sample was

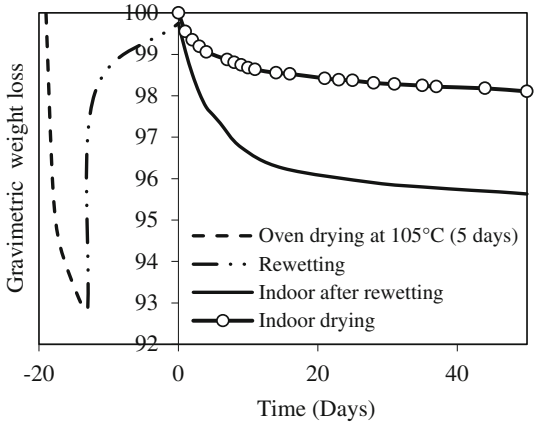

Fig. 10 Effect of drying condition on gravimetric weight loss.

saturated again for 10 days. The rate of gravimetric weight loss after rewetting was compared with the initial drying rate as presented in Fig. 10. As shown, due to oven drying at 105 °C, the microstructure was severely damaged and the rate of gravimetric weight loss increased significantly. In addition, the total weight loss and final degree of saturation was affected. The damage induced during the preconditioning may result in misleading conclusion about the accelerated test results.

3.4 Chloride Permeability and Electrical Restively Results

The total coulombs passed during 6 h of RCP were recorded for the samples with 42 days of water curing. Table 3 shows the classification of concrete for chloride ion penetrability based on total charge passed. As shown in Fig. 11, 50 % GGBS replacement resulted in significant reduction in the total charges passing through the concrete. The concrete samples with 4 and 7 days of water curing were left in indoor condition to measure the natural carbonation rate. After 4 years, the concrete samples were submerged for 10 days to be fully saturated. Figure 12 shows the RCP test results on these samples after 4 years. The total charges passing through the GGBS-blended concrete remained much lower. The total charges passed for GGBS blended concrete samples were approximately 400, 600 and 800 C for w/c = 0.4, 0.5 and 0.6, all in the range of very low according to the classification.

The electrical resistivities of concrete samples were measured using four point Wenner probe technique. As shown in Fig. 13, the electrical resistivity measurements of 50 % GGBS replacement samples were significantly higher than PC samples. Table 4 shows the relationship between electrical resistivity measurement and corrosion rate according to ACI 222R-01 (2001). If the electrical resistivity is larger than 20 kΩ cm, the corrosion rate is slow. For 50 % GGBS replacement, the electrical resistivities were 33, 50 and 72 kΩ cm for w/c = 0.6, 0.5 and 0.4 respectively. The reduction of w/c from 0.6 to 0.4 increased the electrical resistivity by twice, from 11 to around 22 kΩ cm, while replacing 50 % of PC with GGBS for w/c = 0.6 increased the electrical resistivity by three times.

Table 3 Chloride ion penetrability based on charge passed (ASTM C1202-10 2010).

Charge passed (C)	Chloride ion permeability
>4,000	High
2,000–4,000	Moderate
1,000–2,000	Low
100–1,000	Very low
<100	Negligible

Table 4 Relationship between concrete resistivity and corrosion rate (ACI 222R-01 2001).

Resistivity (kΩ cm)	Corrosion rate
>20	Low
10–20	Low to moderate
5–10	High
<5	Very high

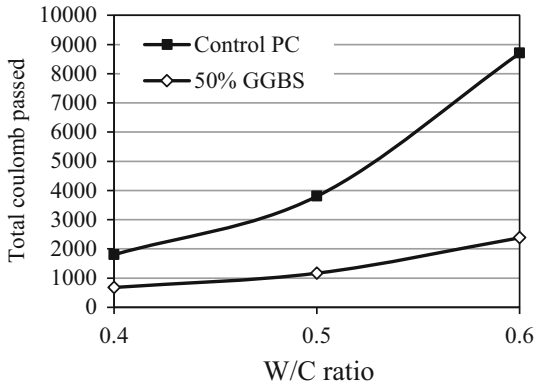

Fig. 11 Effect of w/c ratio on RCPT results (42 days water curing).

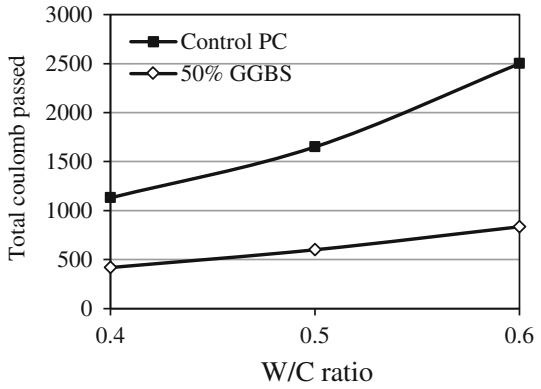

Fig. 12 Effect of w/c ratio on RCPT results (4 years old samples, fully saturated before test and 4–7 days initial curing).

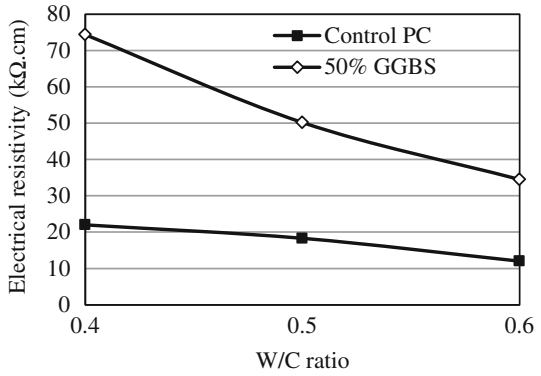

Fig. 13 Effect of w/c ratio on electrical resistivity (4 years old, fully saturated before test and 4–7 days initial curing).

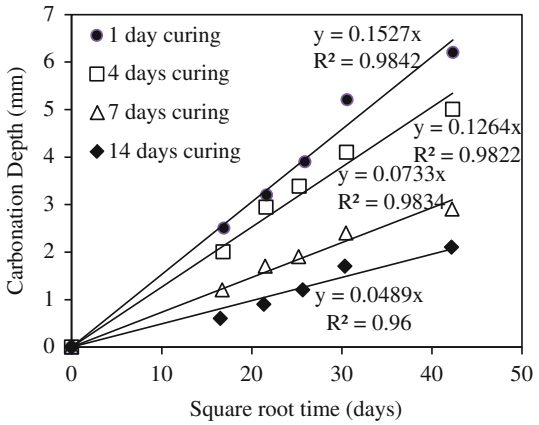

Fig. 14 Effect of curing duration (w/c = 0.5, a/c = 3).

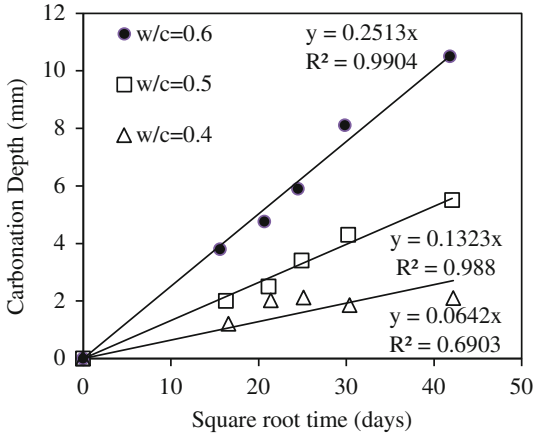

Fig. 15 Effect of w/c ratio (a/c = 4 and 4 days curing).

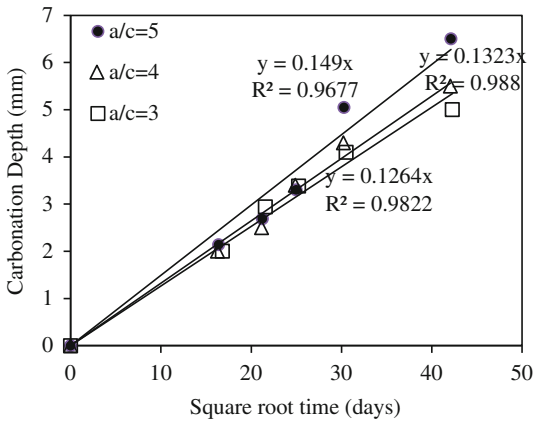

Fig. 16 Effect of a/c ratio (w/c = 0.5 and 4 days curing).

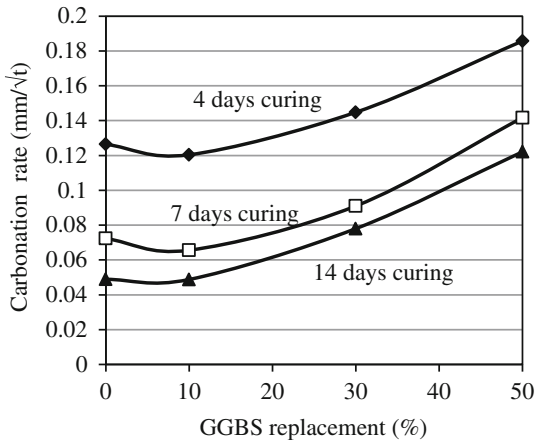

Fig. 17 Effect of GGBS replacement on carbonation rate (w/c = 0.5 and average carbonation rate during 4 years).

3.5 Carbonation Results

The only drawback reported for the GGBS blended cement concrete is the increased rate of carbonation due to consumption of calcium hydroxide. The effects of curing duration, w/c ratio, a/c ratio and GGBS replacement on concrete carbonation are presented in Figs. 14, 15, 16 and 17, respectively. Most of carbonation models predict the carbonation rate to be related to square root of exposure time as follows

$$x = k\sqrt{t}. \tag{2}$$

where x is the depth of carbonation, t is the exposure time and k is a coefficient depending on various factors. Figures 14, 15 and 16 show good correlation of experimental measurements and square root of time. Papadakis (2000) proposed a complete carbonation model considering the type and amount of cementitious materials, degree of hydration and porosity of concrete. However, 105 °C oven drying was used as preconditioning before the carbonation test. As a result, the model overestimates the carbonation rate especially for blended cement concrete (Sabet and Jong 2009). The rate of natural carbonation after 4 years is presented in Fig. 17. As shown, the mix with 10 % GGBS replacement had a carbonation rate similar to that of the PC samples. However, for mixes with 30 and 50 % GGBS replacement, a slight increase in rate of carbonation was observed. As shown in Fig. 14, the rate of carbonation for the concrete sample with 50 % GGBS replacement at 14 days of water curing was slower than PC sample with 4 days of water curing. Therefore, longer curing was required for GGBS blended samples in order to reduce the negative effects.

4. Conclusions

This experiment showed that partial replacement of PC with GGBS improved the pore structure of concrete. The electrical resistivity of the concrete was increased and the total coulombs passed during rapid chloride permeability test were significantly reduced. The rate of carbonation for the samples with 30 and 50 % GGBS replacement increased, however longer period of water curing for GGBS blended cement concrete reduced the carbonation rate and reduce the concern of increased carbonation rate. On top of ecological reasons such as reduced CO_2 foot print and consumption of GGBS (a waste by product of iron production), the GGBS is a viable pozzolanic material for everyday construction purposes considering the improvement in fresh concrete properties, mechanical properties and durability properties.

Open Access

References

ACI Committee 222. (2001). *Protection of metals in concrete against corrosion*. *ACI 222R-01* (pp. 41). Farmington Hills, MI: American Concrete Institute.

ASTM C1202-10. (2010). *Electrical indication of concrete's ability to resist chloride ion penetration*. West Conshohocken, PA: American Society for Testing and Materials.

BS EN 12390-3. (2009). *Testing hardened concrete: Compressive strength of test specimens*. London, UK: British Standards Institute.

Feng, N. Q., Shi, Y. X., & Ding, J. T. (2000). Properties of concrete with ground ultrafine phosphorus slag. *Cement, Concrete, and Aggregates, 22*(2), 128–132.

Galle, C. (2001). Effect of drying on cement-based materials pore structure as identified by mercury intrusion porosimetry: A comparative study between oven-, vacuum-, and freeze. *Cement and Concrete Research, 31*(10), 1467–1477.

Gao, J. M., Qian, C. X., Liu, H. F., Wang, B., & Li, L. (2005). ITZ microstructure of concrete containing GGBS. *Cement and Concrete Research, 35*(7), 1299–1304.

Gjørv, O. E. (2009). *Durability design of concrete structures in severe environments* (p. 232). London, UK: Taylor & Francis.

Güneyisi, E., & Gesoğlu, M. (2008). A study on durability properties of high-performance concretes incorporating high replacement levels of slag. *Materials and Structures, 41*(3), 479–493.

Habert, G., & Roussel, N. (2009). Study of two concrete mix-design strategies to reach carbon mitigation objectives. *Cement & Concrete Composite, 31*(6), 397–402.

Hadj-Sadok, A., Kenai, S., Courard, L., & Khatib, J. M. (2010). Transport properties of mortars and concretes modified with medium hydraulic activity ground granulated blast furnace slags. In *Second International Conference on*

Sustainable Construction Materials and Technologies, Ancona, Italy.

Harrison, T. A., Jones, M. R., Newlands, M. D., Kandasami, S., & Khanna, G. (2012). Experience of using the prTS 12390-12 accelerated carbonation test to assess the relative performance of concrete. *Magazine of Concrete Research, 64*(8), 737–747.

Ji, Y., & Jong, H. C. (2003). Effects of densified silica fume on microstructure and compressive strength of blended cement pastes. *Cement and Concrete Research, 33*(10), 1543–1548.

Jia, Y., Aruhan, B., & Yan, P. (2011). Natural and accelerated carbonation of concrete containing fly ash and GGBS after different initial curing period. *Magazine of Concrete Research, 64*(2), 143–150.

Lagerblad, B. (2005). *Carbon dioxide uptake during concrete life cycle: State of the art*. Swedish Cement and Concrete Research Institute CBI Report 2, ISBN 91-976070-0-2. Stockholm, Sweden: CBI.

Lim, T. Y. D., Sabet, D. B., & Teng, S. (2012). In situ inspection of ultra durable concrete using electrical resistivity technique. *Advanced Materials Research, 368–373*, 1989–1992.

Nazari, A., & Riahi, S. (2011). Splitting tensile strength of concrete using ground granulated blast furnace slag and SiO_2 nanoparticles as binder. *Energy and Buildings, 43*, 864–872.

Papadakis, V. G. (2000). Effect of supplementary cementing materials on concrete resistance against carbonation and chloride ingress. *Cement and Concrete Research, 30*(2), 291–299.

Polder, R. B. (2001). Test methods for onsite measurement of resistivity of concrete: A RILEM TC-154 technical recommendation. *Construction and Building Materials, 15*(2–3), 125–131.

Sabet, D. B., & Jong, H. C. (2006). Effect of preconditioning of concrete under accelerated test. In *31st Conference on Our World in Concrete and Structures* (Vol. 31, pp. 127–134).

Sabet, D. B., & Jong, H. C. (2009). Modeling of carbonation of PC and blended cement concrete. *The IES Journal Part A: Civil and Structural Engineering, 2*(1), 59–67.

Sabet, D. B., Lim, T. Y. D., & Teng, S. (2012). Ultra durable concrete for sustainable construction. *Advanced Materials Research, 368–373*, 553–556.

Shi, H. S., Xu, B. W., & Zhou, X. C. (2009). Influence of mineral admixtures on compressive strength, gas permeability and carbonation of high performance concrete. *Construction and Building Materials, 23*(5), 1980–1985.

Shi, X., Yang, Z., Liu, Y., & Cross, D. (2011). Strength and corrosion properties of Portland cement mortar and concrete with mineral admixtures. *Construction and Building Materials, 25*, 3245–3256.

Shi, X., Xie, N., Fortune, K., & Gong, J. (2012). Durability of steel reinforced concrete in chloride environments: An overview. *Construction and Building Materials, 30*, 125–138.

Teng, S., Lim, T. Y. D., & Sabet, D. B. (2013). Durability and mechanical properties of high strength concrete incorporating ultra fine ground granulated blast-furnace slag. *Construction and Building Materials, 40*, 875–881.

Wang, P. Z., Trettin, R., & Rudert, V. (2005). Effect of fineness and particle size distribution of granulated blast furnace slag on the hydraulic reactivity in cement systems. *Advanced in Cement Research, 17*(4), 161–166.